J. Am. Soc. Mass Spectrom. (2018)
DOI: 10.1007/s13361-018-2034-7

FOCUS: HONORING CAROL V. ROBINSON'S ELECTION TO THE NATIONAL ACADEMY OF SCIENCES: RESEARCH ARTICLE

Solvent Mediation of Peptide Conformations: Polyproline Structures in Water, Methanol, Ethanol, and 1-Propanol as Determined by Ion Mobility Spectrometry-Mass Spectrometry

Tarick J. El-Baba,[1] Daniel R. Fuller,[1] David A. Hales,[2] David H. Russell,[3] David E. Clemmer[1]

[1]Department of Chemistry, Indiana University, 800 Kirkwood Avenue, Bloomington, IN 47401, USA
[2]Department of Chemistry, Hendrix College, Conway, AR 72032, USA
[3]Department of Chemistry, Texas A&M University, College Station, TX 77843, USA

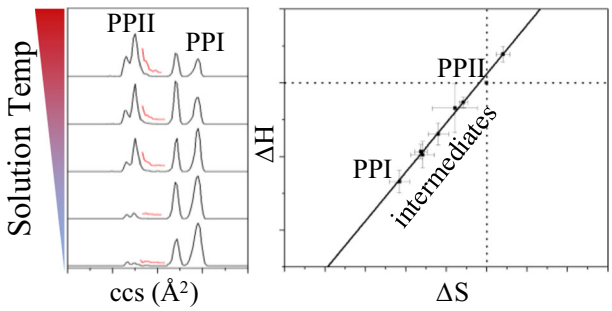

Abstract. Ion mobility spectrometry and circular dichroism spectroscopy are used to examine the populations of the small model peptide, polyproline-13 in water, methanol, ethanol, and 1-propanol over a range of solution temperatures (from 288 to 318 K). At low temperatures, the less-polar solvents (1-propanol and ethanol) favor the all-*cis* polyproline I helix (PPI); as the temperature is increased, the *trans*-configured polyproline II helix (PPII) is formed. In polar solvents (methanol and water), PPII is favored at all temperatures. From the experimental data, we determine the relative stabilities of the eight structures in methanol, ethanol, and 1-propanol, as well as four in water, all with respect to PPII. Although these conformers show relatively small differences in free energies, substantial variability is observed in the enthalpies and entropies across the structures and solvents. This requires that enthalpies and entropies be highly correlated: in 1-propanol, *cis*-configured PPI conformations are energetically favorable but entropically disfavored. In more polar solvents, PPI is enthalpically less favorable and entropy favors *trans*-configured forms. While either ΔH^0 or ΔS^0 can favor different structures, no conformation in any solvent is simultaneously energetically and entropically stabilized. These data present a rare opportunity to examine the origin of conformational stability.

Keywords: Ion mobility spectrometry, Folding, Enthalpy-entropy compensation, Polyproline, Structure, Energetics

Received: 10 April 2018/Revised: 3 July 2018/Accepted: 7 July 2018

Introduction

Characterization of the structures and stabilities of native and non-native forms of polypeptide chains is key to unraveling fundamental aspects of how structure is established [1–6]. However, non-native folds are typically transient in nature [3, 5, 7] and sensitive to the local environment. For example, interactions with solvent, [8–10] small molecules [11–13] (e.g., osmolytes, drugs, lipids) and extreme cases where the polypeptide is imbedded or interacting with membranes [14, 15] can modulate biomolecular structure, increasing the complexity of the folding process. Mass spectrometry, especially "native MS", has emerged as an ideal biophysical tool to study biomolecular structure and interaction [16–19]. When combined with ion mobility spectrometry (IMS), the

Electronic supplementary material The online version of this article (https://doi.org/10.1007/s13361-018-2034-7) contains supplementary material, which is available to authorized users.

Correspondence to: David Clemmer; *e-mail:* clemmer@indiana.edu

Published online: 01 August 2018

IMS-MS technique affords new experimental approaches for understanding how changes in the local environment might alter polypeptide stability and conformational preferences [20].

Oligomers of proline are amongst the most-studied model systems for investigating structure and stability relationships [21–26]; unlike other amino acids, proline-peptide bonds can undergo *cis* ↔ *trans* isomerization [27, 28], which often induces large variations in structure [29]. These bonds are exquisitely sensitive to solvent—favoring the all-*cis* polyproline-I helix (PPI) in 1-propanol and the all-*trans* polyproline-II helix (PPII) in water [30]. The PPI helix is enthalpically stable but entropically disfavored as compared with PPII [22]. Recently, we have characterized eight long-lived structures involved in the PPI↔PPII folding transition of polyproline-13 (Pro13) and examined the mechanisms and pathways for folding [31, 32]. These structures are shown in Scheme 1. When structure A from Scheme 1 (PPI, incubated in 1-propanol) is transferred into water, it undergoes a series of *cis* → *trans* isomerizations at specific peptide bonds in a sequential step-by-step transition through the six intermediates that are shown, to produce structure F (PPII) [31, 32]; the reverse process, in which PPII (incubated in water) is induced to fold to PPI upon immersion in 1-propanol is slower and occurs by a highly parallel mechanism [32].

In this work, we use circular dichroism (CD) spectroscopy and IMS to explore in more detail the role that solvent plays in these transitions by measuring the thermodynamics of the eight Pro13 structures upon incubation in water, methanol, ethanol, or 1-propanol solutions of varying temperature. The combination of techniques allows us to parse out a detailed look at mixtures of conformations that are typically not observable. The outcome is a first glimpse of the interplay between enthalpy and entropy in stabilizing multiple conformations of a biopolymer. From these data, we obtain insight about why specific conformations are favored in some environments while disfavored in others.

Experimental

Synthesis of Pro13

All synthesis reagents were purchased from Midwest Biotech (Indianapolis, IN), except for 3-(diethoxy-phosphoryloxy)-3H-benzo[*d*]-[1,2,3]-triazin-4-one, which was purchased from Aapptec (Louisville, KY). All solvents used were of the highest purity. Pro13 was synthesized using a modified Applied Biosystems 430A synthesizer (Applied Biosystems, Foster City, CA) by standard Boc solid-phase synthesis protocol, and purified by reversed-phase HPLC (> 98% purity), described in detail previously [31].

Sample Preparation and Data Analysis

Stock solutions were prepared in appropriate solvents (water, methanol, ethanol, 1-propanol) to ~ 0.3 mg mL^{-1}. Anhydrous solvents were prepared within 24 h of analysis to ensure samples remained free of water. Working solutions were prepared to 0.03 mg mL (23 μM) and incubated in a water bath for at least 12 h prior to analysis. Mobility distributions were plotted with OriginPro v 9.2.2 (OriginLab Corporation, Northampton, MA) and integrated using the peak analyzer tool. The van't Hoff equation was used to determine the relative energetics for each conformer:

$$\ln(K_{eq}) = -\frac{\Delta H^0}{RT} + \frac{\Delta S^0}{R}$$

where K_{eq} is the value of a conformers equilibrium constant (with respect to conformer F), R is the gas constant, T is the absolute temperature, and ΔH^0 and ΔS^0 are the values of enthalpy and entropy, respectively. Gibbs free energies (ΔG^0) were determined using the Gibbs relationship of $\Delta G^0 = \Delta H^0 - T\Delta S^0$. Values reported are the average of triplicate measurements. Uncertainties are reported as the standard deviation about the mean.

Instrumentation

CD spectroscopy was performed on Jasco J-715 spectrophotometer (Jasco Inc., Easton, MD) using a quartz cuvette with a 1.00-mm optical path length (Hellma Analytics, Plainview, NY). IMS-MS instrumentation [33, 34] and theory [35–37] are described elsewhere; only a brief description of the apparatus is given here. Ions are produced by nano-electrospray ionization (ESI) using a Nanomate Autosampler (Advion, Ithaca, NY) and transferred to the first vacuum stage of the instrument, where they are stored in an hourglass-shaped ion

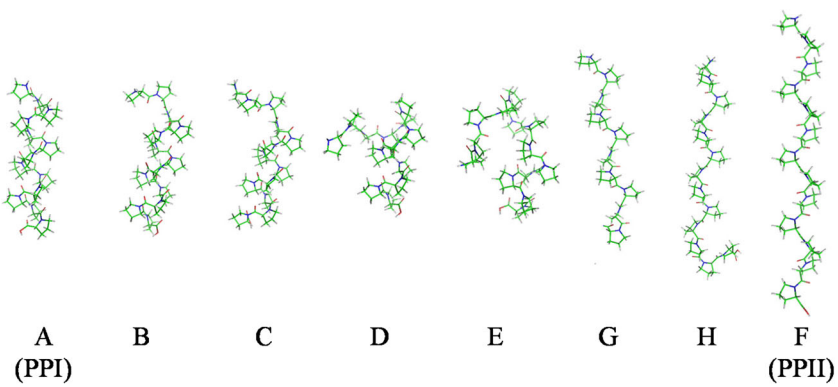

Scheme 1. Ideal polyproline-13 structures (see Table 1 for more details)

funnel [38]. Packets of ions are periodically released into the 2-meter drift tube filled with 3.00 Torr He buffer gas and held at an electric field strength of ~ 10 V cm^{-1}. Ions of varying shapes experience different numbers of collisions with the He buffer gas and therefore, drift at different velocities through the drift tube. Mobility-separated ions exit the drift tube and are pulsed orthogonally into a TOF mass spectrometer for analysis of their mass-to-charge (m/z) ratios. Drift times for peaks corresponding to specific conformations are reproducible from experiment to experiment to within ± 1% relative uncertainty. Thus, we find no evidence for any new structures other than the A through H structures reported previously.

Determination of Experimental Collision Cross Section

IMS separations are recorded as an experimentally-measured drift time (t_d); t_d values are converted to an ion-He collision cross section (CCS) (Ω) using [35]:

$$\Omega = \frac{(18\pi)^{1/2}}{16}\frac{ze}{(k_b T)^{1/2}}\left[\frac{1}{m_I}+\frac{1}{m_B}\right]^{1/2}\frac{t_D E}{L}\frac{760}{P}\frac{T}{273.2}\frac{1}{N}$$

The terms z, e, k_b, and N are the ions' charge, the value of an elementary charge, Boltzmann's constant, and the neutral number density of the buffer gas at standard temperature and pressure. Experimentally controlled parameters of E, L, and P are the electric field strength, the drift tube length, and the absolute pressure of the buffer gas.

Results and Discussion

CD Measurements of Pro13 in Different Solvents

Figure 1 shows CD spectra for Pro13 after incubation in water, methanol, ethanol, or 1-propanol. In water, Pro13 shows a minimum at 205 nm and reaches a maximum signal at 230 nm—the feature at 205 nm is a signature of the all-*trans* PPII helix [22, 23]. A similar (albeit smaller) signal is observed in methanol. The spectrum obtained in ethanol shows minima at 198 and 230 nm and a maximum at 213 nm, indicating the dominant solution-phase population is the *cis*-configured PPI helix [22, 23]. The signals for these signatures increase in 1-propanol. We note that the spectra obtained from ethanol and 1-propanol are similar and consistent with a large population of *cis*-configured peptide bonds. In water and methanol, *trans*-configurations are favored, in agreement with prior CD studies [22, 23].

Combining IMS Measurements with a CD Analysis

While the CD spectra provide information about the average populations of peptide bonds across all structures present in each solution, it does not provide information about contributions from individual conformations. Such insight can be obtained from conformer populations determined by IMS data (when combined with a detailed theoretical analysis of structure) [39, 40]. Briefly, this approach takes advantage of the idea that the mobility of an ion through a buffer gas is related to its shape, which depends on its conformation [16, 41, 42]. Compact conformers have higher mobilities [or smaller collision cross sections (CCS)] than more extended structures [40, 43]. Prior work for doubly protonated Pro13 [31], comparing measured CCSs with values calculated for trial conformations generated by molecular modeling, yielded the eight conformations having *cis* and *trans* peptide bond assignments given in Table 1 and shown in Scheme 1. In Table 1, we expect that the A, B, C, and F *cis*/*trans* assignments should be highly accurate, whereas some variation in the internal peptide bond assignments is expected for D, E, G, and H. The CCSs measured here upon electrospraying from different solvents are identical (within experimental uncertainty) to those reported previously [31]; therefore, we assign these peaks to the A through H conformers, where A corresponds to the all-*cis* PPI helix and F to the *trans*-configured PPII helix.

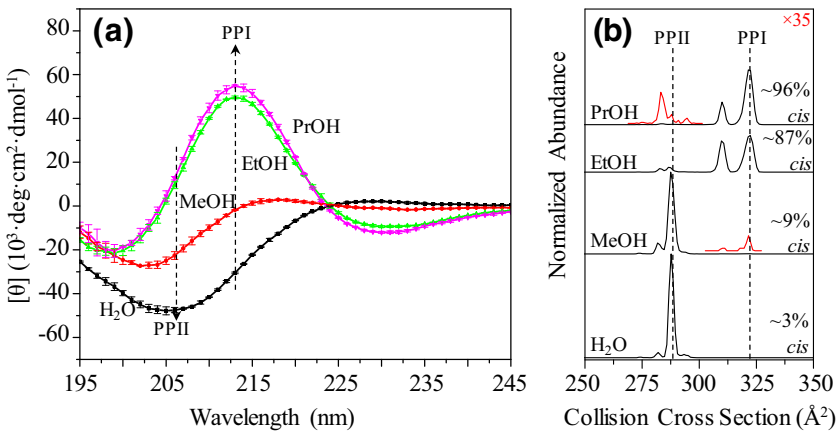

Figure 1. (**a**) CD and (**b**) IMS distributions Pro13 incubated in water, methanol, ethanol, or 1-propanol at 298 K. Inset red lines in (**b**) scaled by × 35

Table 1. Summary of conformer designations, *cis*/*trans* configuration, and experimental and calculated collision cross section (Ω)

Conformer assignment	*cis*/*trans* configuration[a]	Ω_{exp} (Å^2)	Ω_{calc}[a] (Å^2)
A (PPI)	**CCCCCCCCCCCC**	323	324
B	**TTCCCCCCCCCC**	308	309
C	**TTTCCCCCCCCC**	303	306
D	**TTTC**CTCCC**CCC**	298	299
E	**TTTC**CTTCC**CCC**	293	293
G	**TTTTTTTT**CCCC	280	282
H	**TTTTTTTT**TTCT	275	278
F (PPII)	**TTTTTTTTTTTT**	287	288

[a]Configurations and Ω_{calc} values are taken from ref. [31]. Bolded text denoted regions with unambiguous *cis*/*trans* assignments

Consider the IMS distributions for doubly protonated Pro13 originating from these four solvents as shown in Figure 1. In 1-propanol, the IMS distribution is dominated by an intense signal at Ω = 323 Å^2; a slightly more compact structure at Ω = 308 Å^2 is also present. From this distribution, we calculate a weighted-average *cis*-population of ~ 96% for the 1-propanol solution. This is the first analysis to delineate the average populations measured from a CD experiment as composites of multiple conformations, rather than a portion of an ensemble of different conformational types. In this case, the ~ 4% population of trans-configured bonds from the bulk system arises from the B conformation, having two *trans*-peptide bonds in its structure and comprising ~ 30% of the IMS distribution.

Upon electrospraying from ethanol, we observe that the abundance of conformer B is nearly equivalent to that for A. Several low-abundance signals centered at Ω = 287 Å^2 are also present, corresponding to the PPII helix (conformer F) and other *trans*-configured structures that have collapsed in vacuo upon removal of solvent, as assigned previously [31]. The IMS distributions from methanol and water are almost identical. The methanol solution contains only trace amounts of the PPI structure and conformers B, and C, and in water, these are not observed. Overall, the populations that are extracted from the IMS data (and *cis*/*trans* structural assignments) are in good agreement with the conformationally unresolved changes observed for different solvents by CD, corroborating our prior assignments.

Equilibrium Thermochemistry for Different Conformations in Different Solvents

By measuring the populations of structures from the IMS distributions for samples that are incubated at varying solution temperatures, it is possible to measure the equilibrium thermochemistry of these different structures in each solution. As an example, Figure 2 shows IMS distributions for Pro13 incubated in ethanol at various solution temperatures. At 293 K, the PPI helix is most abundant. The distribution is similar at 298 K, and at 303 K, the signal for PPII is nearly equal to that for PPI and conformer B. The population shifts to favor PPII and other structures with a high degree of *trans*-configured prolyl bonds as the temperature is increased to 313 K. These observations are also consistent

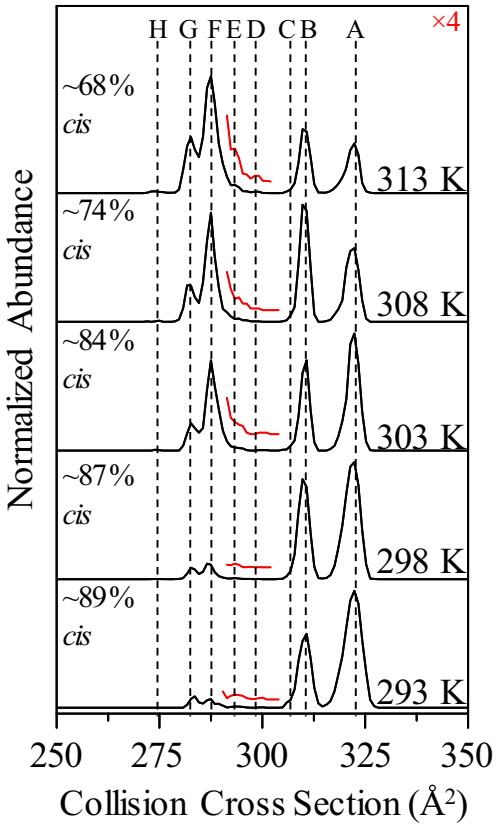

Figure 2. IMS distributions obtained from ethanol at representative solution temperatures. Inset red lines scaled by × 35

with prior CD studies [22, 23], demonstrating that PPII, and other conformers dominated by *trans*-configured peptide bonds are stable at high temperatures. From these data, we see that these states must be entropically preferred. The IMS populations from water, methanol, and 1-propanol also show subtle variations in conformer abundances with changes in solution temperature (see Supporting Information).

A summary of the relative thermochemistry for the A through H conformers in each solvent, calculated from the enthalpies (ΔH^0) and entropies (ΔS^0), determined from van't Hoff plots (see Figure S2 and Tables S1–S4 in the Supporting Information) of the temperature-dependent IMS populations is shown in Figure 3. All thermochemical values are determined with respect to PPII (conformer F). The values of ΔG^0 show that PPI is most stable relative to other structures in 1-propanol and becomes less favored in ethanol and methanol. We anticipate that the PPI helix, and structures having large fractions of *cis*-configured peptide bonds, also follow this trend; however, these structures are presumably too unstable to be observed in water. The only conformers observed in water (conformers D, E, G, and H, Table 1), are less stable than PPII. In methanol, only small amounts of PPI are observed (ΔG^0 ~ 14 kJ mol^{-1}) and even smaller fractions of states B and C are apparent; instead, methanol appears to stabilize structures with increasing fractions of *trans*-configured bonds, with the all-*trans* PPII helix being most preferred. In ethanol and 1-propanol, all the other structures are less stable than PPI.

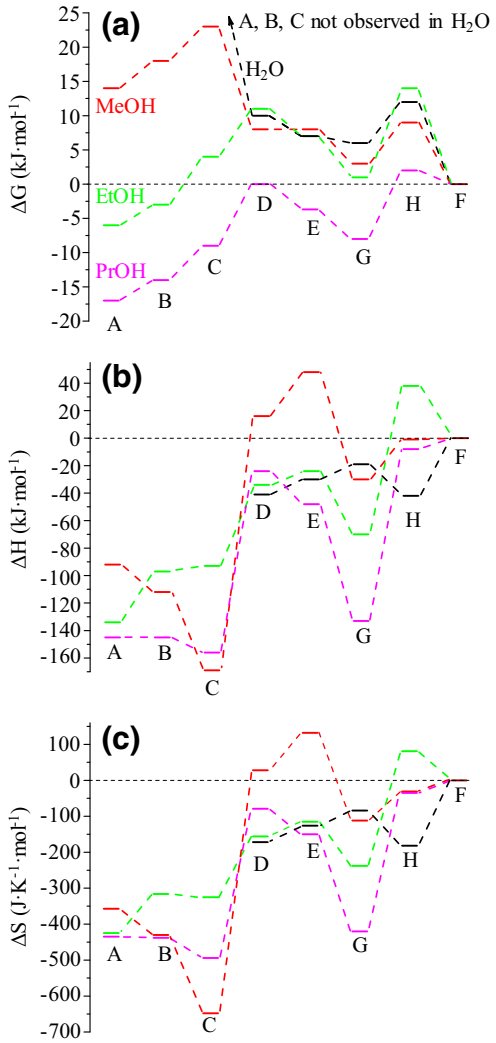

Figure 3. (**a**) ΔG^0, (**b**) ΔH^0, and (**c**) ΔS^0 diagrams for each conformation, all plotted relative to conformer F (PPII) determined in water, methanol (MeOH), ethanol (EtOH), and 1-propanol (PrOH) solutions. Values plotted are the average of triplicate measurements. All values and uncertainties (standard deviation about the mean) are reported in the supporting information (Tables S1–S4)

Understanding the Origins of Relative Stabilities

An understanding of the origins of conformer stabilities can be obtained by examining the ΔH^0 and ΔS^0 diagrams (see Figure 3). We begin by comparing the relative enthalpies. PPI is enthalpically most favored (relative to other structures) in 1-propanol. The relative enthalpy of this structure approaches zero with increasing solvent polarity, and PPI is not observed in water. Structures with mainly *cis*-peptide bonds (PPI, conformers B and C) are ~90–160 kJ mol^{-1} more enthalpically favorable than PPII. Examination of all ΔH^0 values reveals that PPII is the least enthalpically stable structure, except for conformers D and E from methanol solutions and conformer H from ethanol, which are minor features in their respective mobility distributions. In summary, virtually all-*cis*-configured prolyl bonds are stabilized by ΔH^0 as compared to *trans*-oriented structures. For PPI, the backbone carbonyl oxygens are aligned parallel to the backbone and directed toward the positively charged N-terminus resulting in a strong helical macrodipole moment that stabilizes this structure relative to PPII. In this configuration, there are few ways that solvent can form hydrophilic interactions (e.g., hydrogen bonds, salt bridges) with the peptide backbone; weak hydrophobic interactions (e.g., van der Waals) between the solvent must provide some enthalpic stability to PPI.

Figure 3 shows ΔS^0 values for each conformer. Consider the entropic component of PPI in each solvent. PPI is the least entropically favored configuration in 1-propanol, followed closely by PPI in ethanol and then methanol. By extrapolating the apparent dependence on solvent polarity, it can be assumed that PPI and other *cis*-configured structures are entropically more favorably stable in water, even though they are not experimentally observed. Despite the energetic favorability of PPI, and conformers B and C, they are quite entropically disfavored (ΔS^0 ~ −350 to −650 J K^{-1} mol^{-1}) compared to PPII. In PPII, the backbone carbonyls are perpendicular to the backbone which exposes hydrophilic regions that can interact with neighboring polar solvent—such intermolecular interactions are the stabilizing interactions that favor PPII.

Enthalpies and Entropies for Intermediates Are Highly Correlated

Figure 4 shows plots of intermediate thermochemistry extracted from these data. As we examined these plots, we were struck that in each solvent, the energetics associated with these conformations shows a strong correlation of enthalpy and entropy. Correlation plots of ΔH^0 and ΔS^0 values for small molecule chemical reaction systems as well as larger biological molecules that exhibit two-state, cooperative folding, and unfolding transitions have been observed previously [44–50]. From our thermochemistry, it appears that this correlation is not only important at the endpoints of a two-state process or reaction, but also for many other stable conformations. This is significant. Many of the structures observed in our equilibrium distributions for different solvents are transient intermediates in previous folding studies. Thus, our data provides experimental evidence that this balance of stabilizing forces appears to be important throughout the conformational landscape.

Additional insight about structural stabilization can be obtained by thinking about four quadrants (Q_1 through Q_4) that any structure could reside in (Figure 4). In Q_1, ΔH^0 and ΔS^0 are both unfavorable; any structure that persists in this space would do so despite unfavorable energetics. Structure found in Q_2 are favored by ΔS^0, but ΔH^0 unfavorable; in Q3, ΔH^0 is favorable and ΔS^0 is disfavored; and, structures in Q_4 are stabilized by both ΔH^0 and ΔS^0.

We begin by considering the implications that no conformations are ever found in Q_1 or Q_4. It makes sense that both enthalpic and entropic interactions should disfavor conformations and thus it is not surprising that no structures are

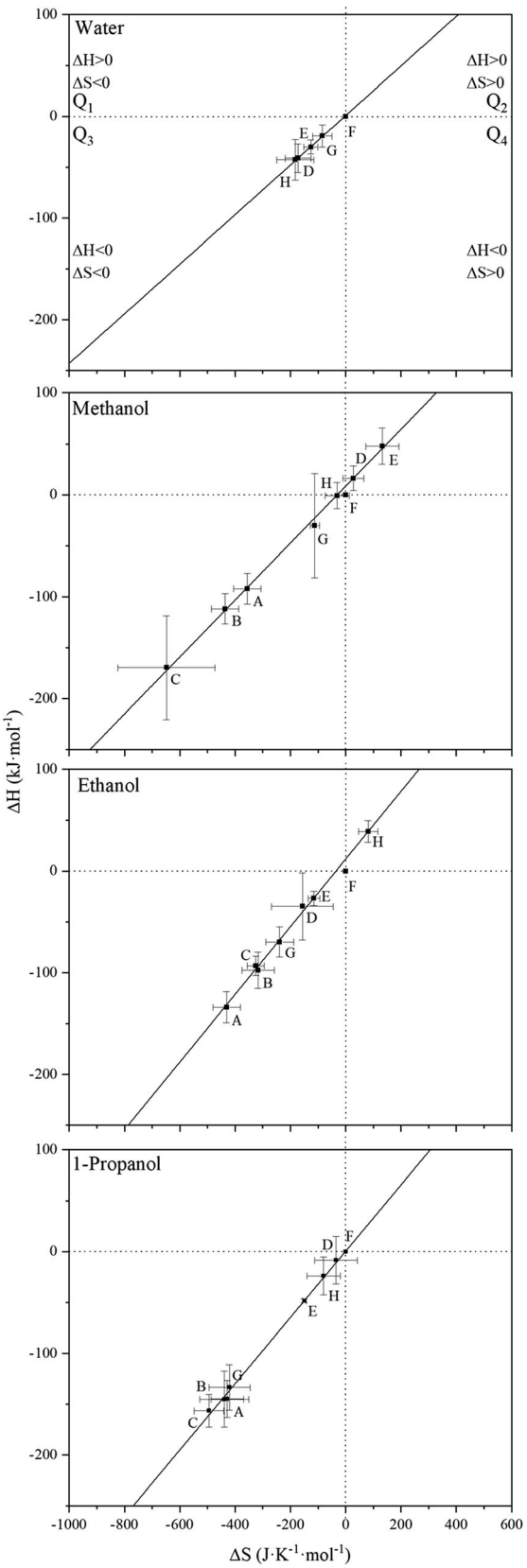

Figure 4. Enthalpy-entropy diagrams for each solvent system investigated. Quadrants (Q_1–Q_4) delineate thermodynamically preferred terms as shown in the figure (see text for more details). Each value is the average of triplicate measurements, and error bars represent the standard deviation about the mean

found in Q_1. However, at first glance, one might think that Q_4 would be most populated with structures, since both entropic and enthalpic interactions would be favored. However, for this to be true, a structure would require many relatively tight enthalpically favoring bonding interactions, while the system becomes relatively structurally dynamic (i.e., sampling a wide conformational space or many transient solvent-conformation interactions). No structures are observed in this region because tight-binding interactions apparently restrict increased dynamics associated with increasing the entropy. Our data show that the energetic terms for each conformation fall into Q_2 and Q_3, an indication that these dynamic species rely on the delicate balance between ΔH^0 and ΔS^0 to undergo folding.

Enthalpies and Entropies for Transition States Are Also Highly Correlated

The analysis presented in this work has encouraged us to return to our earlier kinetics studies where we followed the transitions of either PPI → PPII or PPII → PPI. In the former case, PPI is prepared by incubating Pro13 in 1-propanol. The transition was initiated by rapid dilution into water to a final solution concentration of 90:10 water:1-propanol. The latter PPII → PPI transition was initiated by diluting PPII (prepared by incubating Pro13 in water) with 1-propanol to a final composition of 97:3 1-propanol:water solution. An enthalpy-entropy correlation plot for these systems is shown in Figure 5. Because we determined the temperature-dependent rates for the observed structural transitions, we were also able to extract transition state thermochemistry. These data are also included in Figure 5. While the thermochemistry is somewhat different in the mixed solvent systems, we find a strong enthalpy-entropy correlation amongst the precursors and intermediate states that are observed. But, importantly the transition states also show this correlation. Prior work indicated that the PPI → PPII transition was sequential [31] (i.e., A → B → C → D → …) whereas the PPII → PPI transition occurred by a parallel mechanism [32]. The plots in Figure 5 show that regardless of the pathway (sequential vs parallel), there is a strong correlation of enthalpy and entropy. This result is striking as it shows that transition states as well as intermediates are defined by a complex interplay between thermodynamic forces. As one thinks about all of the many interactions within the peptide as well as environment that may vary along a complex structural rearrangement, it is perhaps not surprising that the forces governing these changes are highly correlated. In this way, the conformations and systems work together to establish the favored distributions of coexisting states.

Summary and Conclusion

Studies of the solvent-dependent thermochemistry of Pro13 was determined using CD and IMS. The data support prior evidence that the all-*trans* PPII helix is preferred in polar solvents (water and methanol) and that the *cis*-configured PPI helix is favored in less polar solvents (ethanol and 1-propanol). PPI, having *cis*-

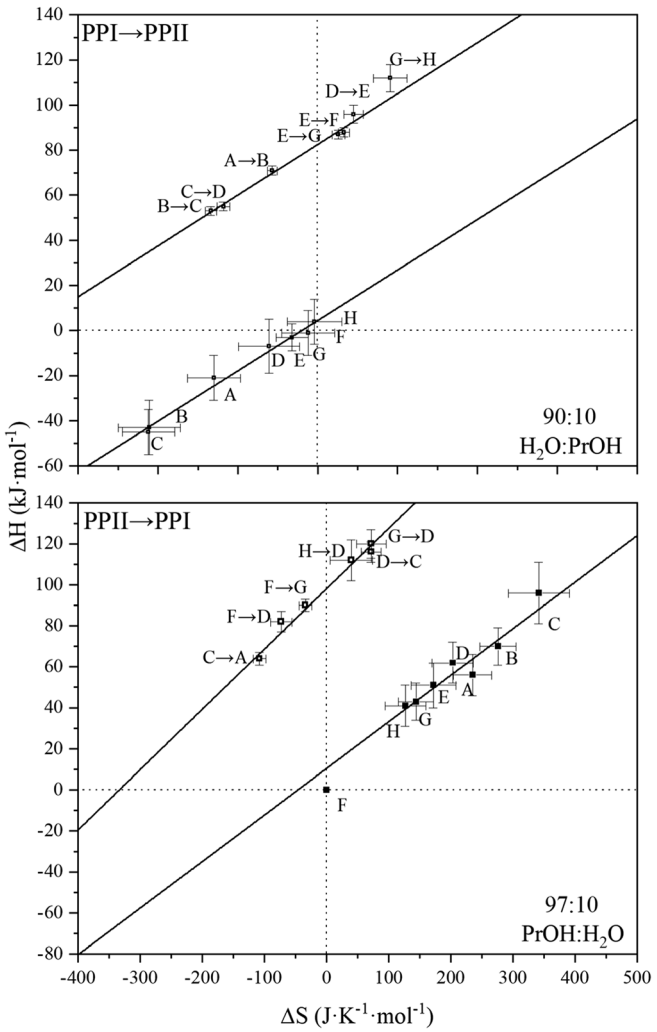

Figure 5. Enthalpy-entropy diagrams for 90:10 1-propanol:H_2O and 97:3 H_2O:1-propanol. Open and closed symbols denote values for transition state and equilibrium thermochemistry, respectively. See text for more details. Each value is the average of triplicate measurements, and error bars represent the standard deviation about the mean. Values are taken from ref. [32]

configured peptide bonds is enthalpically favored, whereas PPII and *trans*-oriented prolyl bonds are favored by entropy. The energetic and entropic terms for the different conformations, as well as transition states are highly correlated, regardless of folding pathway or environment. This is an important result to observe experimentally, especially for so many states as it shows that there is a complex balance of forces that governs the distributions of structures that are present in different environments. It appears that peptides take advantage of the flexibility of many interactions as a means of establishing the final structural distribution within an environment.

Acknowledgements

T. J. E. acknowledges support from the Robert and Marjorie Mann Graduate Fellowship from Indiana University.

Funding information

This work was supported in part by funds from the Waters Corporation, the National Institutes of Health R01 GM117207-03 and R01 GM121751-01A1, and the Robert and Marjorie Mann endowment.

References

1. Dill, K.A., Chan, H.S.: From leventhal to pathways to funnels. Nat. Struct. Biol. **4**, 10–19 (1997)
2. Dill, K.A., Ozkan, S.B., Shell, M.S., Weikl, T.R.: The protein folding problem. Annu. Rev. Biophys. **37**, 289–316 (2008)
3. Daggett, V., Fersht, A.R.: The present view of the mechanism of protein folding. Nat. Rev. Mol. Cell Biol. **4**, 497–502 (2003)
4. Dill, K.A., MacCallum, J.: The protein-folding problem, 50 years on. Science. **338**, 1042–1046 (2012)
5. Englander, S.W., Mayne, L.: The nature of protein folding pathways. Proc. Natl. Acad. Sci. U. S. A. **111**, 15873–15880 (2014)
6. Gruebele, M., Dave, K., Sukenik, S.: Globular protein folding in vitro and in vivo. Annu. Rev. Biophys. **45**, 233–251 (2016)
7. Neudecker, P., Lundstrom, P., Kay, L.E.: Relaxation dispersion NMR spectroscopy as a tool for detailed studies of protein folding. Biophys. J. **96**, 2045–2054 (2009)
8. Pierson, N.A., Chen, L., Valentine, S.J., Russell, D.H., Clemmer, D.E.: Number of solution states of bradykinin from ion mobility and mass spectrometry measurements. J. Am. Chem. Soc. **133**, 13810–13813 (2011)
9. Shi, H., Clemmer, D.E.: Evidence for two new solution states of ubiquitin by IMS-MS analysis. J. Phys. Chem. B. **118**, 3498–3506 (2014)
10. Wyttenbach, T., Bowers, M.T.: Structural stability from solution to the gas phase: native solution structure of ubiquitin survives analysis in a solvent-free ion mobility-mass spectrometry environment. J. Phys. Chem. B. **115**, 12266–12275 (2011)
11. Han, L., Ruotolo, B.T.: Hofmeister salts recover a misfolded multiprotein complex for subsequent structural measurements in the gas phase. Angew. Chem. **52**, 8329–8332 (2013)
12. Marcoux, J., Champion, T., Colas, O., Wagner-Rousset, E., Corvaia, N., Van Dorsselaer, A., Beck, A., Cianferani, S.: Native mass spectrometry and ion mobility characterization of trastuzumab emtansine, a lysine-linked antibody drug conjugate. Protein Sci. **24**, 1210–1223 (2015)
13. Laganowsky, A., Reading, E., Allison, T.M., Ulmschneider, M.B., Degiacomi, M.T., Baldwin, A.J., Robinson, C.V.: Membrane proteins bind lipids selectively to modulate their structure and function. Nature. **510**, 172–175 (2014)
14. Patrick, J.W., Gamez, R.C., Russell, D.H.: The influence of lipid bilayer physicochemical properties on gramicidin a conformer preferences. Biophys. J. **110**, 1826–1835 (2016)
15. Gupta, K., Donlan, J.A.C., Hopper, J.T.S., Uzdavinys, P., Landreh, M., Struwe, W.B., Drew, D., Baldwin, A.J., Stansfeld, P.J., Robinson, C.V.: The role of interfacial lipids in stabilizing membrane protein oligomers. Nature. **541**, 421–424 (2017)
16. Wyttenbach, T., Pierson, N.A., Clemmer, D.E., Bowers, M.T.: Ion mobility analysis of molecular dynamics. Annu. Rev. Phys. Chem. **65**, 175–196 (2014)
17. Lanucara, F., Holman, s.W., Gray, C.J., Eyers, C.E.: The power of ion mobility-mass spectrometry for structural characterization and the study of conformational dynamics. Nat. Chem. **6**, 281–294 (2014)
18. Lossl, P., van de Waterbeemd, M., Heck, A.J.R.: The diverse and expanding role of mass spectrometry in structural and molecular biology. EMBO J. **35**, 2634–2657 (2016)
19. Eschweiler, J.D., Kerr, R., Rabuck-Gibbons, J., Ruotolo, B.T.: Sizing up protein-ligand complexes: the rise of structural mass spectrometry approaches in the pharmaceutical sciences. Annu. Rev. Anal. Chem. **10**, 25–44 (2017)
20. Clemmer, D.E., Russell, D.H., Williams, E.R.: Characterizing the Conformationome: towards a structural understanding of the proteome. Acc. Chem. Res. **50**, 556–560 (2017)
21. Torchia, D.A., Bovey, F.A.: A nuclear magnetic resonance study of poly(L-proline) in aqueous and aqueous salt solutions. Macromolecules. **4**, 246–251 (1971)

22. Kuemin, M., Schweizer, S., Ochsenfeld, C., Wennemers, H.: Effects of terminal functional groups on the stability of the polyproline II structure: a combined experimental and theoretical study. J. Am. Chem. Soc. **131**, 15474–15482 (2009)
23. Kuemin, M., Engel, J., Wennemers, H.: Temperature-induced transition between polyproline I and II helices: quantitative fitting of hysteresis effects. J. Pept. Sci. **16**, 596–600 (2010)
24. Korter, T.M., Zeitler, J.A., Orlando, R., Sibik, J., Ruggiero, M.T.: Measuring the elasticity of poly-l-proline helices with terahertz spectroscopy. Angew. Chem. Int. Ed. **55**, 6877–6881 (2016)
25. Moradi, M., Babin, V., Roland, C., Sagui, C.: A classical molecular dynamics investigation of the free energy and structure of short polyproline conformers. J. Chem. Phys. **133**, 125104–125122 (2010)
26. Lin, Y.J., Chu, L.K., Horng, J.C.: Effects of terminal aromatic residues on polyproline conformation: thermodynamic and kinetic studies. J. Phys. Chem. B. **119**, 15796–15806 (2015)
27. Fasman, G. D.: Poly-α-amino acids. Dekker, New York (1967).
28. Schimmel, P.R., Flory, P.J.: Conformational energy and configurational statistics of poly-L-proline. Proc. Natl. Acad. Sci. U. S. A. **58**, 52–59 (1967)
29. Andreotti, A.H.: Native state proline isomerization: an intrinsic molecular switch. Biochemistry. **42**, 9515–9524 (2003)
30. Forsythe, K.H., Hopfinger, A.J.: The influence of solvent on the secondary structures of poly(L-alanine) and poly(L-proline). Macromolecules. **6**, 423–437 (1973)
31. Shi, L., Holliday, A.E., Shi, H., Zhu, F., Ewing, M.A., Russell, D.H., Clemmer, D.E.: Characterizing intermediates along the transition from polyproline I to polyproline II using ion mobility spectrometry-mass spectrometry. J. Am. Chem. Soc. **136**, 12702–12711 (2014)
32. Shi, L., Holliday, A.E., Glover, M.S., Ewing, M.A., Russell, D.H., Clemmer, D.E.: Ion mobility-mass spectrometry reveals the energetics of intermediates that guide polyproline folding. J. Am. Soc. Mass Spectrom. **27**, 22–30 (2016)
33. Merenbloom, S.I., Koeniger, S.L., Valentine, S.J., Plasencia, M.D., Clemmer, D.E.: Anal. Chem. **78**, 2802–2809 (2006)
34. Koeniger, S.L., Merenbloom, S.I., Valentine, S.J., Jarrold, M.F., Udseth, H., Smith, R.D., Clemmer, D.E.: Anal. Chem. **78**, 4161–4174 (2006)
35. Mason, E.A., McDaniel, E.W.: Transport properties of ions in gases. Wiley, New York (1988)
36. Shvartsburg, A.A., Jarrold, M.F.: Chem. Phys. Lett. **261**, 86–91 (1996)
37. Mesleh, M.F., Hunter, J.M., Shvartsburg, A.A., Schatz, G.C., Jarrold, M.F.: J. Phys. Chem. **100**, 16082–16086 (1996)
38. Shaffer, S.A., Tang, K.Q., Anderson, G.A., Prior, D.C., Udseth, H.R., Smith, R.D.: Rapid Commun. Mass Spectrom. **11**, 1813–1817 (1997)
39. von Helden, G., Hsu, M.T., Kemper, P.R., Bowers, M.T.: J. Chem. Phys. **95**, 3835–3837 (1991)
40. Jarrold, M.F., Constant, V.A.: Phys. Rev. Lett. **67**, 2994–2997 (1991)
41. Clemmer, D.E., Jarrold, M.F.: Ion mobility measurements and their applications to clusters and biomolecules. J. Mass Spectrom. **32**, 577–592 (1997)
42. Jarrold, M.F.: Unfolding, refolding, and hydration of proteins in the gas phase. Acc. Chem. Res. **32**, 360–367 (1999)
43. Jarrold, M.F.: Helices and sheets in vacuo. Phys. Chem. Chem. Phys. **9**, 1659–1671 (2007)
44. Constable, F.H.: The mechanism of catalytic decomposition. Proc. R. Soc. London, Ser. A. **108**, 355–388 (1925)
45. Thorn, R.J.: Correlation of enthalpy and entropy in sufficiently equivalent systematic errors, vaporization of uranium. J. Chem. Phys. **52**, 474–476 (1970)
46. Liu, L., Guo, Q.X.: Isokinetic relationship, isoequilibrium relationship, and enthalpy-entropy compensation. Chem. Rev. **101**, 673–695 (2001)
47. Jen-Jacobson, L., Engler, L.E., Jacobson, L.A.: Structural and thermodynamic strategies for site-specific DNA binding proteins. Structure. **8**, 1015–1023 (2000)
48. Pan, A., Biswas, T., Rakshit, A.K., Moulik, S.P.: Enthalpy–entropy compensation (EEC) effect: a revisit. J. Phys. Chem. B. **119**, 15876–15884 (2015)
49. Sharp, K.: Entropy-enthalpy compensation: fact or artifact? Protein Sci. **10**, 661–667 (2001)
50. Chodera, J.D., Mobley, D.L.: Entropy-enthalpy compensation: role and ramifications in biomolecular ligand recognition and design. Annu. Rev. Biophys. **42**, 121–142 (2013)